



Review

Distinctive Oxide Films Develop on the Surface of FeCrAl as the Environment Changes for Nuclear Fuel Cladding

Haozheng Qu *, Liang Yin , Michael Larsen and Raul B. Rebak *

GE Vernova Advanced Research Center, Schenectady, NY 12118, USA; liang.yin@ge.com (L.Y.); larsen@ge.com (M.L.)

* Correspondence: haozheng.qu@ge.com (H.Q.); rebak@ge.com (R.B.R.)

Abstract: The corrosion-resistant properties of IronChromium–Aluminum (FeCrAl) alloys have been known for nearly a century. Since the 1950s, they have been explored for application in the generation of nuclear power. In the last decade, the focus has been on the use of FeCrAl as cladding for uranium dioxide fuel in light water reactors (LWRs). The corrosion resistance of this alloy depends on the oxide that it can develop on the surface. In LWRs in the vicinity of 300 °C, the external surface oxide of the FeCrAl cladding could be rich in Fe under oxidizing conditions but rich in Cr under reducing conditions. If there is an accident and the cladding is exposed to superheated steam, the cladding will protect itself by developing an alpha aluminum film on the surface.

Keywords: FeCrAl; fuel cladding; surface oxides; oxidizing and reducing conditions



Citation: Qu, H.; Yin, L.; Larsen, M.; Rebak, R.B. Distinctive Oxide Films Develop on the Surface of FeCrAl as the Environment Changes for Nuclear Fuel Cladding. *Corros. Mater. Degrad.* **2024**, *5*, 109–123. <https://doi.org/10.3390/cmd5010006>

Academic Editors: Angeliki G. Lekatou and Jamie Quinton

Received: 31 January 2024

Revised: 9 March 2024

Accepted: 11 March 2024

Published: 18 March 2024



Copyright: © 2024 by the authors. Licensee MDPI, Basel, Switzerland. This article is an open access article distributed under the terms and conditions of the Creative Commons Attribution (CC BY) license (<https://creativecommons.org/licenses/by/4.0/>).

1. Introduction

Iron–Chromium–Aluminum (FeCrAl) alloys were first developed almost a century ago. For many decades, FeCrAl alloys were mostly used for heating elements in electric furnaces because of their extraordinary resistance to attack by air and steam at temperatures higher than 1000 °C. Their resistance to further oxidation was due to the development, on the surface of the elements, of a one-micrometer-thick aluminum oxide film, which did not allow for oxygen diffusion to the underlying matrix. Since the 1950s, FeCrAl alloys have been explored for nuclear applications, such as cladding for fuel, mainly because of their resistance to environmental interactions and their superior mechanical properties at temperatures of 600 °C and higher. The fuel rod in a light water reactor (LWR) includes ceramic fuel pellets of uranium dioxide (UO₂) encased in a tube or cladding made of a metallic alloy. Since the late 1950s, the cladding in LWRs was mostly based on the element zirconium (Zr) due to its higher transparency to thermal neutrons. Extensive research has been conducted in the last 60+ years on the behavior of Zr alloys in the entire fuel cycle, from cradle to grave. The tsunami-induced accident at the Fukushima Daiichi nuclear power stations in 2011 reminded the international nuclear materials community to reconsider FeCrAl alloys as a more robust cladding alternative for UO₂ fuel. In the last decade, there has been an international effort to assess the performance of FeCrAl as cladding in the LWR-like environment fuel cycle. Most of the effort has been spent on showing the superior behavior of FeCrAl to Zr cladding under accident conditions (mainly above 1000 °C in steam). However, the cladding will very rarely experience accident conditions in the reactor; however, the cladding will certainly experience all the temperatures and environments typical of a fuel cycle including tube fabrication, normal operation in the reactor, shutdown conditions (e.g., during refueling), and used fuel management. Figure 1 shows schematically the range of temperatures that the FeCrAl cladding may be exposed to while being used to generate power at LWR plants. Figure 1 shows that the most likely temperatures will range from ambient conditions to approximately 300 °C. Very rarely or never would the temperatures be higher than 400 °C. Like most other corrosion-resistant alloys, FeCrAl relies on the formation of surface oxides to defend itself from the

environment. FeCrAl alloys are sometimes called smart alloys since they create, on their surface, different oxides depending on the environment they are experiencing.

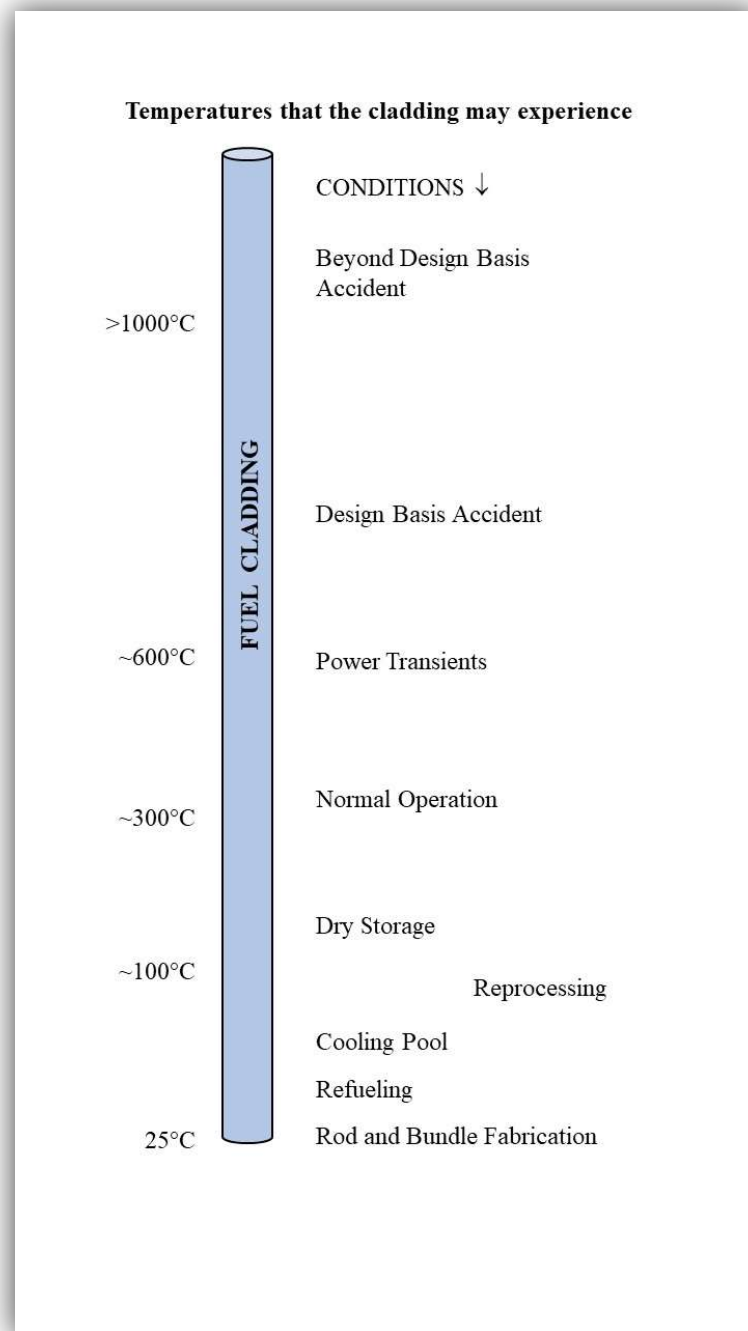


Figure 1. Temperatures that a fuel cladding may experience. At each temperature, the environment may be different.

The objective of this manuscript was to present a literature review to understand what type of oxides may develop on the surface of FeCrAl cladding tubes, particularly FeCrAl ODS, APMT and C26M, in the simulated LWR conditions outlined in Figure 1, which are the conditions that the cladding may be exposed to during the fuel cycle. The data shown in this review are cited from the currently available literature supplemented by archival data from GEVAR on this specific and narrow topic. This manuscript does not review the

oxides that may develop on other nuclear materials such as austenitic stainless steels and nickel-based alloys.

2. Rod and Bundle Fabrication

Table 1 shows some of the most common FeCrAl alloys that are being studied worldwide as part of accident-tolerant fuel (ATF) programs. The most consistent compositions reported in the literature are for PMC26M and APMT2, which are being investigated at General Electric and other research organizations. FeCrAl ODS and variations are being investigated in Japan and have also maintained a consistent composition throughout the last quinquennium. PMC26M and APMT2 alloys are currently made by powder metallurgy through an extrusion process into hollow precursors and then pilgered into thin wall tubes [1]. The current geometry of these FeCrAl tubes is typical of Boiling Water Reactor (BWR) applications, with an approximately 10 mm OD and 0.3 mm wall thickness. Any other geometry can be manufactured as desired. The currently envisioned fuel bundle fabrication process would be similar to that for Zr alloys such as Zircaloy-2, that is, a clean tube of approximately 4 m long is adapted with a welded cap in one end, then filled with the desired UO₂ fuel pellets and then a final cap will be welded to hermetically seal the rod at the other end. Many welding processes may work but the one currently preferred by the industry is pressure resistance welding, which does not involve melting. FeCrAl alloys are ferritic stainless-steel-like alloys, that is, they contain sufficient chromium to develop a native Cr-rich oxide film on the surface at ambient temperature in air. No one has been reported to characterize the thickness and composition of the native oxides formed in air at ambient temperature on the surface of the alloys in Table 1. Besides the commercial compositions in Table 1, many other variations of Cr, Al, molybdenum (Mo), and yttrium (Y) have been studied.

Table 1. Nominal composition of FeCrAl alloys candidate for ATF cladding in weight percent. Balance is Fe.

Alloy	Cr	Al	Others
C26M	12	6	2Mo, 0.2Si, 0.03Y
APMT	21	5	3Mo, 0.4Mn, 0.7Si
FeCrAl ODS	12	6	0.5Ti, 0.4Zr, 0.5Y ₂ O ₃
APM	21	5.8	0.7Si, 0.4Mn
Aluchrom Y Hf	20	6	0.1Y, 0.1Hf, Si, Mn

3. Oxidation of FeCrAl Cladding under LWR Normal Operation Conditions

Once the fuel bundles are fabricated and delivered to nuclear power stations by fuel vendors, they are kept in nearly pure water pools at near ambient temperature. Once the bundles are arranged into the reactor core, the temperature of the cladding will be raised to the vicinity of 300 °C (or normal operation conditions) to produce steam.

In BWRs, the steam is produced directly above the reactor core, but in pressurized water reactors (PWRs), the steam is produced in a steam generator outside the reactor core. Normally, after two years or so, approximately one-third of the bundles from the core may be discharged and replaced with fresh fuel bundles and the other two-thirds of the bundles may be rearranged into the core. In this process of fueling and refueling, the cladding temperature may experience temperature changes from near ambient to the vicinity of 300 °C (Figure 1) and then back to near ambient during the next refueling. Each bundle may experience at least three such cycles during their useful life producing steam. There are no data on the oxide film thickness or composition that may develop on the surface of the FeCrAl cladding following three cycles in a commercial LWR core under irradiation.

Experiences from out-of-pile autoclave testing (for example, in cycles of three months and then cooling down to ambient temperature and then raising again to near 300 °C for

another three months) show that the oxide formed at a high temperature remains stable at near ambient temperature. The initial information available from the literature regarding oxide formation on FeCrAl cladding involves out-of-pile exposure at temperatures near the operation conditions of 300 °C. The structure of the oxides on FeCrAl has been studied to some extent as a function of temperature, exposure time, water composition, and FeCrAl alloy composition [2–6].

4. General Corrosion of FeCrAl Alloys in Out-of-Pile Autoclave Tests at ~300 °C

The structure (thickness and composition) of the oxides will be discussed based on influencing factors such as (a) internal (e.g., the FeCrAl composition) and (b) external or environmental (e.g., if the water is oxidizing or reducing, dissolved species in water, pH, and temperature effects in the vicinity of 300 °C). Several years of testing experience has shown that the most important variables controlling the dissolution of FeCrAl in water at nearly 300 °C are the redox potential (oxygen vs. hydrogen) and the amount of Cr in the alloy [2,7]. When the gas in the ~300 °C water is changed from less than 1 ppm hydrogen to 1 ppm oxygen, the corrosion potential of FeCrAl alloys can change by more than 600 mV [8]. When the corrosion potential is high (oxidizing), the FeCrAl alloys (even the ones with 12–13%Cr) would passivate and offer a low dissolution or recession rate. When the corrosion potential is low (reducing or with hydrogen gas), the mass loss by FeCrAl alloys is higher (and a higher mass loss for the lower Cr alloys) [2,7].

Autoclave exposure tests have been conducted to determine the rate of corrosion, or the dissolution of the FeCrAl material mostly in the ~300 °C range in water (generally between 288 °C and 360 °C). The first and more complete sets of tests were conducted at (a) the General Electric Corrosion and Electrochemistry Laboratory (now GE Vernova Advanced Research or GEVAR) [2], (b) at the Oak Ridge National Laboratory [9,10], and (c) at the Nippon Fuel Development or NFD laboratories [11]. Immersion tests conducted at GE were typically in three autoclave conditions: (a) PWR, high-purity water at 330 °C containing 3.75 ppm of dissolved hydrogen; (b) BWR, hydrogen water chemistry (HWC), high-purity water at 288 °C containing 0.3 ppm of dissolved hydrogen; and (c) BWR, normal water chemistry (NWC), high-purity water at 288 °C containing 1 ppm of dissolved oxygen.

The mass change behavior of FeCrAl coupons in ~300 °C water has a direct relationship with their capacity to passivate [2]. The passivation in ~300 °C water is mostly controlled by the content of Cr in the FeCrAl alloy. The higher the Cr content (e.g., APMT), the better the passivation [2]. For example, Qu et al. [12] tested coupons of five different FeCrAl alloys containing from 7%Cr to 13%Cr for four months under PWR-type conditions at 360 °C in a static autoclave and they reported that the higher the Cr content in the alloy, the lower the mass gain by the coupon, meaning that the higher-Cr alloy passivated more quickly and did not allow for oxide growth. In oxidizing conditions like in BWR normal water chemistry (NWC) at 288 °C, the FeCrAl coupons practically do not undergo a mass change even after immersion for a year [2,11]. In reducing conditions, such as BWR hydrogen water chemistry (HWC) at 288 °C, the FeCrAl coupons tend to gradually suffer a uniform recession in their thickness; the lower the Cr content in the FeCrAl, the higher the recession (dissolution) rate in HWC [2,11,13,14].

5. Composition of the Oxides Developed on FeCrAl in Out-of-Pile Autoclave Tests at ~300 °C

The composition and thickness of the oxide on the surface of the FeCrAl cladding is different depending on if the redox potential is reducing (hydrogen water chemistry HWC) or oxidizing (normal water chemistry NWC [7]). Under reducing conditions, the oxides on the surface would be mainly Cr₂O₃ and single-layered. Under oxidizing conditions, the surface oxide is a double layer, with a thicker external layer rich in Fe and Cr and a thinner inner layer rich in Cr. After a year of immersion in near 300 °C water under NWC, APMT starts to enrich in Al underneath the Cr oxide film. It is not clear yet how the presence of Mo in the FeCrAl alloys affects their passivation behavior at near 300 °C.

5.1. Oxides under Oxidizing Conditions (BWR NWC)

Figure 2 shows the FIB and TEM cross-section of the oxide films developed on the OD surface of APMT tubing exposed for 12 months to out-of-pile BWR NWC in 288 °C water containing 1 ppm dissolved oxygen (O₂). The total thickness of the oxide film is approximately 300 nm and formed mainly by two layers, an external one constituted mostly of Fe and Cr and an internal one which is Cr-rich (Figure 2a). The inner portion of the internal oxide layer rich in Cr also contains some aluminum. Figure 2b shows that underneath the continuous Cr-rich oxide layer, there is a non-continuous enrichment in Al, which seems to be in the non-oxidized matrix, which is sometimes called the transition layer [15]. Figure 3 shows the thickness and composition of the oxide developed on the surface of a C26M tube specimen after one year of immersion in BWR NWC conditions. The oxide film on C26M under BWR NWC is like that developed on APMT but thinner. Yin et al. [2] reported slightly more mass loss for the C26M coupons than for the APMT coupons in BWR NWC conditions. Figure 3 shows the two-layer oxide on C26M; the external is enriched in Fe and the thinner internal layer contains Cr and Al. Similar findings were reported by Yamashita et al. [16].

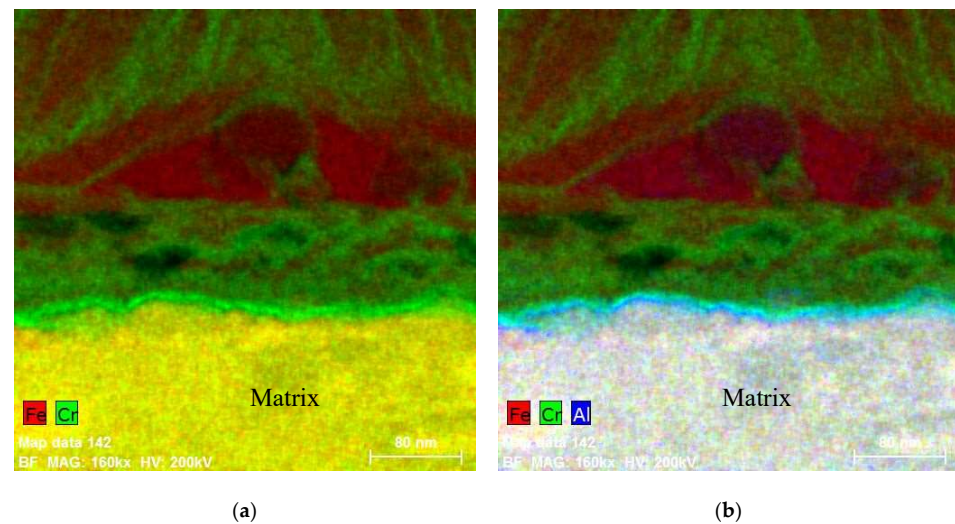


Figure 2. Oxide films developed on the surface of APMT cladding tube after 12-month exposure to BWR NWC water at 288 °C containing 1 ppm O₂. (a) Fe and Cr EDS composite map; (b) Fe, Cr and Al EDS composite map.

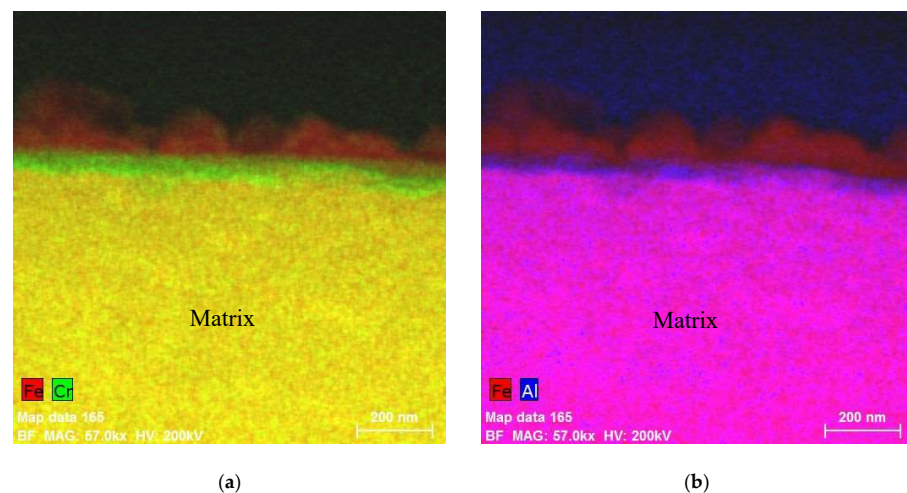


Figure 3. Oxide films developed on the surface of C26M cladding tube after 12-month exposure to BWR NWC water at 288 °C containing 1 ppm O₂. (a) Fe and Cr EDS composite map; (b) Fe and Al EDS composite map.

5.2. Oxides Developed under Reducing Conditions (BWR HWC and PWR)

Figures 4 and 5 show, respectively, the oxide characteristics developed, respectively, on APMT and C26M coupons after 12-month immersion in BWR HWC. Figure 4a shows that the oxide film that developed on APMT tube specimen was mostly one layer rich in Cr and containing Al. The Al was mostly enriched at the boundary between the oxide and the matrix. On top of the oxide layer, there were some isolated crystals rich in Fe (which may have developed by reprecipitation from the recirculating autoclave water). Figure 5a shows that the oxide that developed on the C26M tube specimen was mostly one layer rich in Cr. The inner portion of this Cr-rich oxide layer also contained Al (Figure 5a,b). Compared with Figure 4 for APMT, the top of the oxide does not contain crystals rich in Fe, probably because the recession rate of C26M was faster than that of APMT in BWR HWC and would not allow for the crystals to develop, or the developed crystals would fall off [2]. Figure 5 also shows that the oxide on C26M was thicker than the oxide on the APMT (Figure 4), probably because the lower Cr in C26M makes it more difficult to passivate.

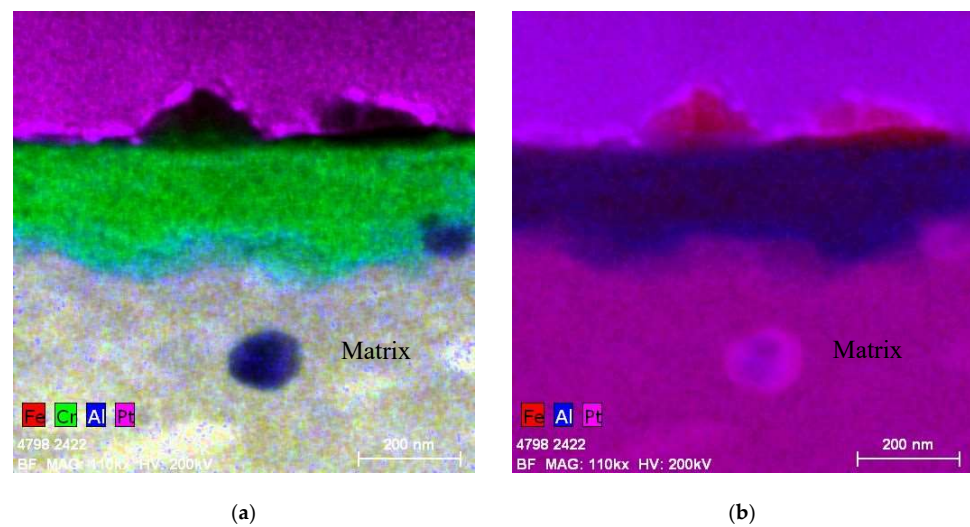


Figure 4. Oxide films developed on the surface of APMT cladding tube after 12 months' exposure to BWR HWC water at 288 °C containing 0.3 ppm H₂. (a) Fe, Cr, Al and Pt EDS composite map; (b) Fe, Al and Pt EDS composite map.

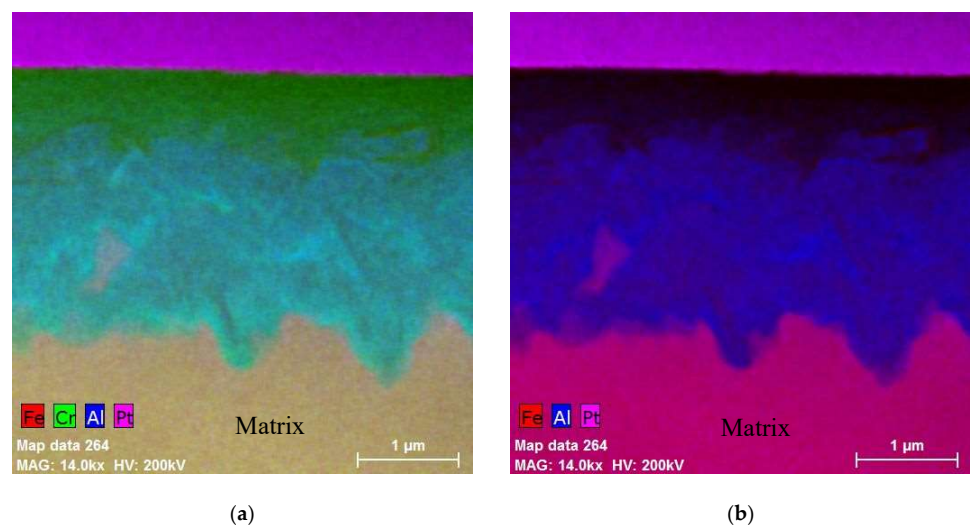


Figure 5. Oxide films developed on the surface of C26M cladding tube after 12 months' exposure to BWR HWC water at 288 °C containing 0.3 ppm H₂. (a) Fe, Cr, Al and Pt EDS composite map; (b) Fe, Al and Pt EDS composite map.

Figures 6 and 7 show the oxide films developed, respectively, on the APMT and C26M tubes in PWR environments at 330 °C. In PWR environments both alloys lost some mass, twice as much in C26M than in APMT [2]. Compared with the other reducing environment (BWR HWC), the mass loss in PWR conditions was smaller than in BWR HWC conditions [2]. Figure 6a shows that the oxide developed on APMT in PWR conditions was mostly rich in Cr but also contained Al. Compared to Figure 4a, the oxide on APMT in PWR was thinner than in BWR HWC conditions. As it was argued before, the higher temperature in PWR may have accelerated the passivation for the high Cr APMT [2]. Figure 7 shows that the oxide on top of C26M tubes in PWR environment was thicker than the oxide on APMT (Figure 6). On C26M the oxide was Cr-rich with two distinguishable regions, like the oxide in BWR HWC (Figure 5). The most external region of the Cr rich oxide did not contain Al, while the internal thicker region did contain Al. Comparing Figures 5 and 7, the oxide under BWR HWC on C26M was thicker than in PWR conditions. Again, it is likely that under PWR conditions, C26M was able to offer better passivation and therefore lower corrosion rates [2].

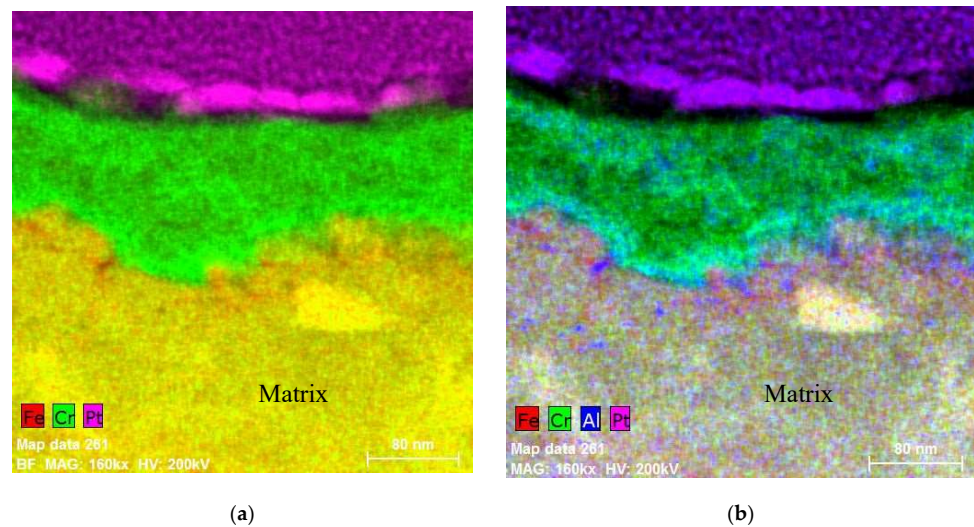


Figure 6. Oxide films developed on the surface of APMT cladding tube after 12 months' exposure to PWR water at 330 °C containing 3.75 ppm H₂. (a) Fe, Cr and Pt EDS composite map; (b) Fe, Cr, Al and Pt EDS composite map.

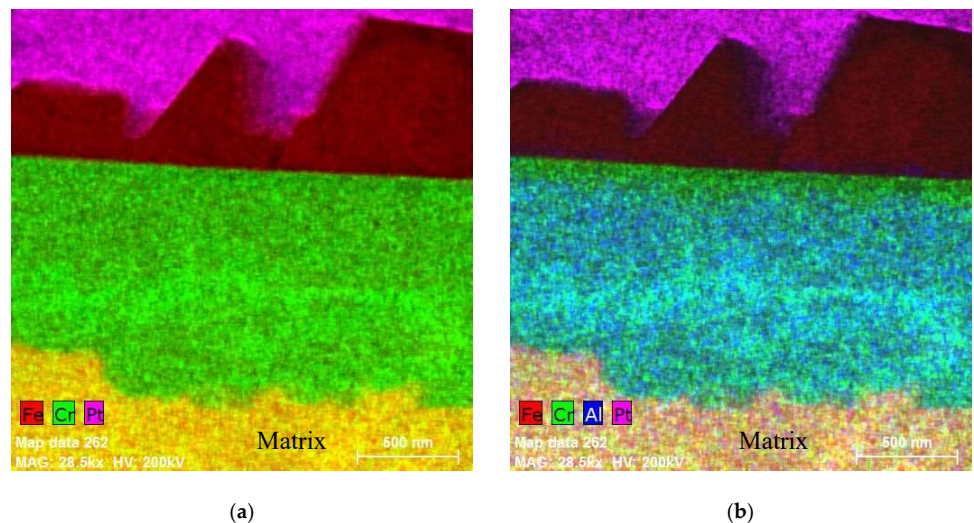


Figure 7. Oxide films developed on the surface of C26M cladding tube after 12 months' exposure to PWR water at 330 °C containing 3.75 ppm H₂. (a) Fe, Cr and Pt EDS composite map; (b) Fe, Cr, Al and Pt EDS composite map.

The presence of Al enrichment underneath the Cr-enriched oxide has also been reported by Terrani et al. [13] for one year's exposure of a model (non-commercial) alloy (Fe-10Cr-5Al) under PWR reducing conditions. Al enrichment under the Cr-rich oxide was also observed for an Fe-10Cr-5Al model alloy tested for one year under BWR NWC conditions but no Al enrichment was detected for the specimens tested under BWR HWC conditions [13]. It is likely that the higher recession rate under BWR HWC would not allow sufficient time for Al to be enriched since the oxide may be dissolving in the reducing water faster as it develops. For a higher-Cr FeCrAl such as APMT, the presence of the Al-enriched zone does not seem to be present for coupons tested for 6 months [17]. It may take longer than 6 months for the enrichment of Al to be established. Raiman et al. [14] reported Al enrichment underneath the Cr-rich oxide after 9 months of immersion of APMT and model alloy C35M3 coupons in BWR NWC, but they did not report Al enrichment underneath the Cr-rich oxide for APMT and C35M3 coupons immersed for 9 months under BWR HWC. This again could be related to the less protective oxide film that develops in BWR HWC. It has also been observed that when the Cr content is in the lower range (e.g., 12–13%), the aluminum does not enrich in the transition layer between the Cr oxide and the matrix, but the Al enrichment is in the Cr oxide itself [12]. An illustrative summary of oxide formation after 12-month exposure to simulated LWR water conditions is shown in Figure 8.

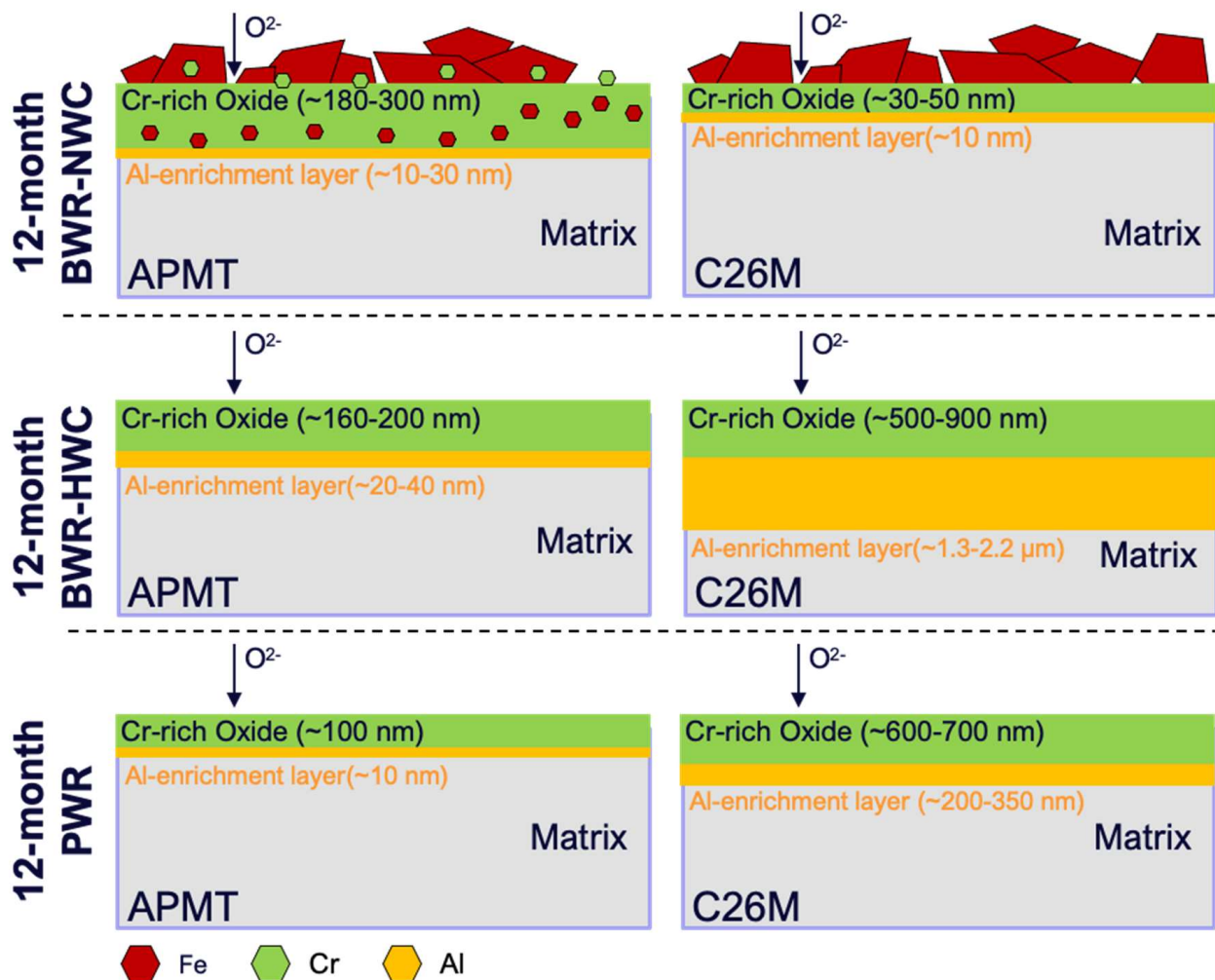


Figure 8. Oxide films developed on the surface of APMT and C26M cladding tubes after 12 months' exposure to three LWR conditions.

Besides the work conducted at GE, ORNL, and at NFD, the FeCrAl alloys have also been tested in China and other countries but not in a highly systematic manner. A review

article by Jiang et al. [18] listed the double layer oxides formed under BWR NWC (with dissolved oxygen) on FeCrAl coupons. They reported that the external layer was an Fe-rich spinel sometimes containing nickel (Ni) (Ni is not present in FeCrAl alloys but may still be present in the test water because of minor dissolution from the stainless steel piping and autoclave body). The presence of Al in the transition region between the Cr-rich oxide and the base metal was also reported by Was et al. [19] and Ning et al. [15] at higher tested temperatures of 320 °C and 360 °C, respectively. After testing tubes of Fe-13Cr-5Al for 100 days under PWR conditions, Ning et al. [15] reported Al enrichment in the Cr-rich oxide. The findings by Ning et al. [15] were also corroborated by Qu et al. [12] after testing 7–13% Cr FeCrAl for 4 months at 360 °C.

6. Oxide Film Development during Accident Conditions

6.1. Design-Basis Accident Conditions (DBA)

The NRC defines DBA as a postulated accident that a nuclear facility must be designed and built to withstand without loss to the systems, structures, and components necessary to ensure public health and safety. That is, this is a recoverable accident condition. It is not clear in an LWR what the temperature of the fuel bundles during a DBA would be, but the environment could probably be steam at a temperature below 800 °C. Roy et al. [6] studied the oxide film developed on model alloys when they were exposed to steam at 400 °C for 100 h. They reported that when Fe-17Cr-4Al was exposed to steam at 400 °C for 100 h, the total surface oxide was approximately 200 nm thick with an external layer rich in Fe and an internal layer approximately 20 nm thick rich in Cr towards the outside and enriched in Al towards the matrix. These results in steam at 400 °C closely follow the behavior of the oxide structures reported in condensed water at about 100 °C lower temperatures [6]. The main difference is that, in steam, the external mostly Fe-rich oxide cannot disperse or dissolve in condensed water like in the tests at the lower temperatures of ~300 °C. Qu et al. [20] tested the model alloy Fe-21Cr-5.5Al-3Mo in steam at 400 °C for 100 h. The analysis of the surface showed an oxide approximately 1 µm thick, containing two layers. The external thicker layer contained Fe and Mo and the internal thinner layer was Cr-rich and enriched in Al [20]. The presence of Mo in the alloy showed a detrimental effect on the protectiveness of the oxide film that developed in steam at the lower temperature of 400 °C. The presence of Mo in the alloy does not seem to affect the oxidation resistance of FeCrAl in steam at temperatures higher than 1000 °C. Moreover, Mo may provide a beneficial effect on strengthening the mechanical properties of FeCrAl.

6.2. Beyond Design-Basis Accidents (BDBA)

The NRC defines BDBA as a technical way to discuss accident sequences that are possible but were not fully considered in the design process because they were judged to be too unlikely. (In that sense, they are considered beyond the scope of design-basis accidents that a nuclear facility must be designed and built to withstand.) As the regulatory process strives to be as thorough as possible, “beyond design-basis” accident sequences are analyzed to fully understand the capability of a design. It is assumed that a reactor core damage is unrecoverable from a BDBA. Examples of these BDB accidents include Fukushima in 2011 and Chernobyl in 1986. FeCrAl alloys were initially selected as candidates for the cladding of the uranium-based fuel because of their extraordinary resistance to attack by steam at temperatures higher than 1000 °C [9]. FeCrAl alloys made by traditional metallurgy (melting and forging) and by powder metallurgy showed extraordinary resistance to attack by steam if the amount of Cr and Al in the alloy met some minimum values [21,22]. Most of the >1000 °C tests were performed for a few hours. Recently, it was demonstrated that neutron-irradiated defueled FeCrAl cladding was also resistant to attack by steam at 1200 °C [23].

It has been shown repeatedly in the last decade that FeCrAl alloys, with enough Cr and Al, develop a 1 µm thick layer of columnar alpha alumina on the surface when exposed to steam at temperatures higher than 1000 °C [9,24]. If the oxidation is performed

in plain air (see next section), the oxide may not be a single layer of columnar alpha alumina. Rebak et al. [25] did a systematic study of the effect of the temperature on the oxidation characteristics of APMT and C26M in air and in steam between 800 °C and 1300 °C. The behavior of C26M was like the behavior of APMT both in air and in steam [25]. Lipkina et al. [26] studied the oxidation behavior of FeCrAl ODS (12Cr-6Al) in air and steam up to 1400 °C, and they reported a thicker alumina oxide on the surface in the presence of air than in steam. It is likely that in steam, the alumina oxide develops faster and then the matrix does not suffer further oxidation due to the protectiveness of the alumina film. In air, the oxide may seem less protective (more defective), allowing for oxygen to diffuse through the oxide and allowing it to grow thicker.

Figure 9 shows the oxide characteristics developed on APMT after 4 h of exposure at 1200° to laboratory air [25]. The oxide layer on the surface was basically two layers of pure alumina 1 to 2 μm thick. The external alumina layer was less than 10% of the total thickness and contained mostly smaller grains, while the internal thicker layer was columnar alpha alumina. Between the two alumina layers, there was some residual trapped Cr. It is likely that when the coupon was being heated in air, first, a Cr-rich oxide developed and then as the temperature increased, the alumina that developed underneath the Cr oxide pushed through, trapping some of the Cr before the Cr would be consumed by reaction with the steam contained in the air. The white dots in the oxide show porosity, probably because of the removal of trapped Cr. This surface oxide does not contain either Fe or Mo.

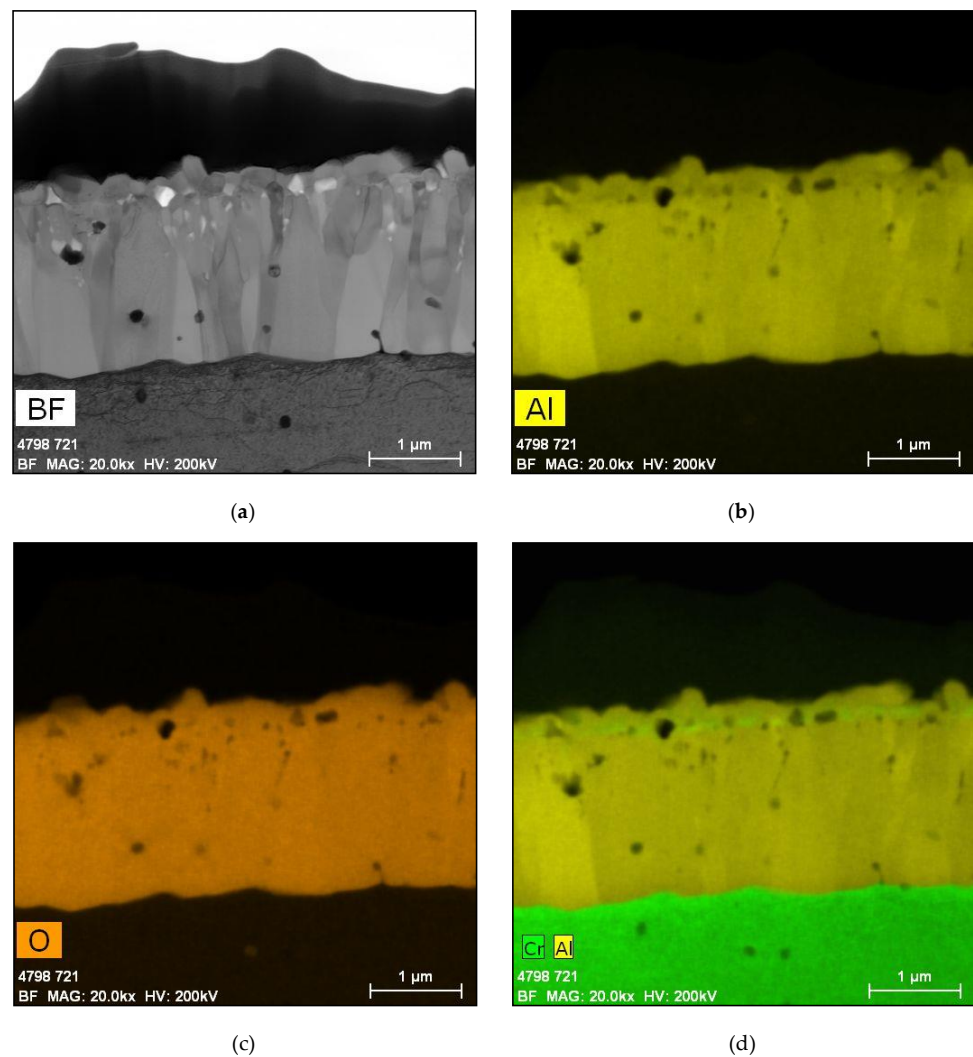


Figure 9. Oxide film developed on the surface of APMT after 4-h exposure to air at 1200 °C. Adapted from ref. [25]. (a) BF-TEM image; (b,c) Al and O EDS maps; (d) Cr and Al EDS composite map.

Figure 10 shows the oxide that developed on the surface of APMT when exposed for 4 h to pure steam at 1200 °C [25]. The oxide is a single layer of columnar alumina less than 1 μm thick. In pure steam, there is a large availability of water gas in the chamber which can quickly remove the initial Cr oxide from the surface, allowing for the growth of a pure protective (no porosity) alumina layer. This surface oxide does not contain either Fe or Mo.

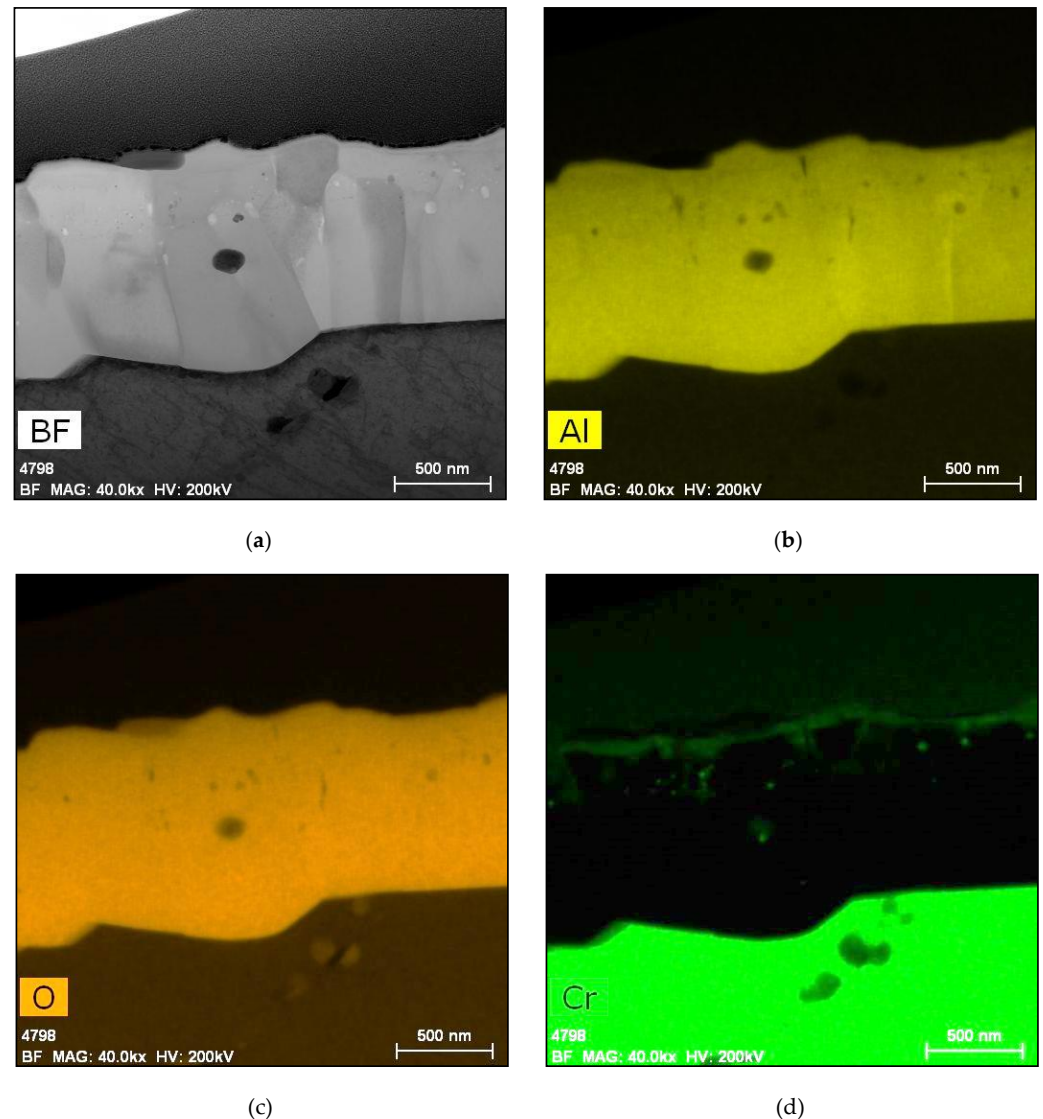


Figure 10. Oxide film developed on the surface of APMT after 4-h exposure to air at 1200 °C. Adapted from ref. [25]. (a) BF-TEM image; (b–d) Al, O and Cr EDS maps.

7. FeCrAl Alloy Oxidation Behavior in Other Environments

7.1. Industrially Pre-Oxidized APMT in Air

Some FeCrAl alloys can be purchased commercially in the pre-oxidized condition. Industrially, pre-oxidation is conducted in air at 1050 °C for 8 h. It has been shown before that when the oxidation of APMT is conducted in pure steam at 1200 °C, the surface oxide is a single layer approximately 1 μm thick of columnar pure alpha alumina. However, when the oxidation is performed in air for 8 h at the slightly lower temperature of 1050 °C, there are two distinctive layers of oxide. Figure 11a,b show the total oxide thickness is between 500 nm and 1 μm and is practically pure alumina (Figure 11c,d). The distinctive external layer is approximately one-fourth of the total oxide thickness and it is less structurally defined than the internal layer approximately three-fourths of the oxide thickness. There is no iron in the oxide developed in air at 1050 °C. Figure 11f shows that a small amount

of Cr is retained between the two layers of alumina rich oxide. It is likely that at the lower temperatures (during heating up in the furnace in air), the surface of the APMT was covered by Cr oxide, and as the temperature increased, alumina started to develop and pushed through the Cr oxide. As the temperature progressed above 1000 °C, and for the next 8 h, another alumina layer grew underneath the first layer (the larger columnar oxide of the inner layer in Figure 11a,b). Since the heating was performed in air and not in steam, the air does not contain sufficient water molecules to react with the Cr oxide and evaporate it as a hydroxide. This is the reason why the remnants of Cr oxide are trapped between the two layers of alumina in Figure 11.

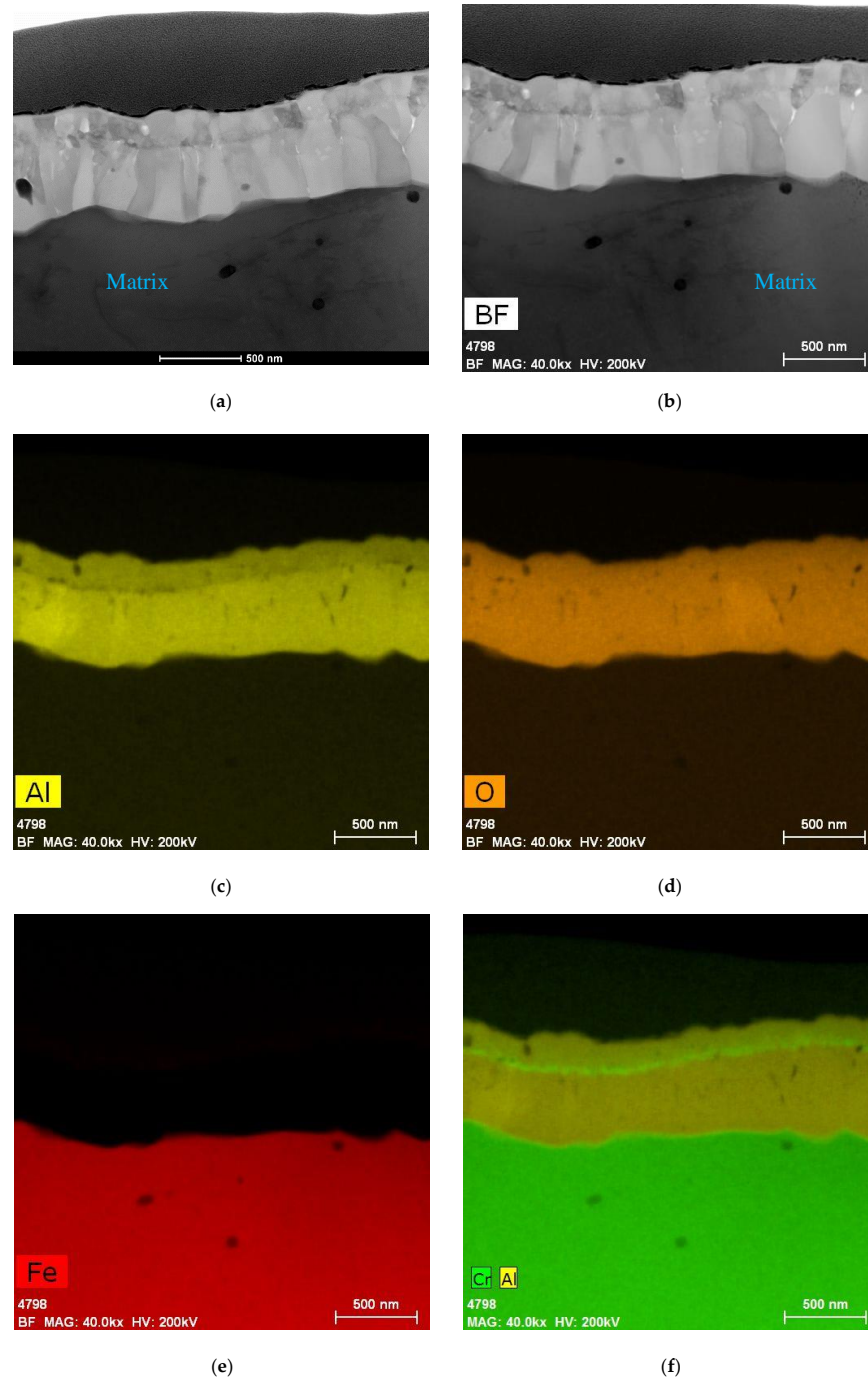


Figure 11. Oxide films developed on the surface of APMT sheet after 8-h exposure at 1050 °C in air. (a,b) BF-TEM image; (c–e) Al, O and Fe EDS maps; (f) Cr and Al EDS composite map.

7.2. Passive Behavior of FeCrAl in Cooling Pools

Spent fuel pools or cooling pools are methods used in nuclear power stations to decrease the radioactivity of used fuel rods by storing them under approximately 6 m of well-controlled chemistry water. The water acts as an agent to remove the heat from the radioactive rods and provides radiation shielding for anyone near the pool. Used rods generally may spend up to 20 years in cooling pools before being transported to dry cask storage. The temperature of the water in the pool could be in the range of 60 °C and has a strictly regulated pH and chloride concentration. The water conditions may change depending on if the cladding is Zr-based or FeCrAl. The conditions of the water in the pools are benign for stainless materials such as FeCrAl, which have sufficient Cr ($\geq 12\%$) to render them stainless or passive. Electrochemical tests were performed using APMT, C26M, FeCrAl ODS and type 304SS tubes at ambient, 45 °C and 60 °C in 3.5% NaCl environments [17]. Electrochemical impedance spectroscopy testing showed that all the tested materials remained passive. The highest polarization resistance (R_p) values in 3.5% NaCl at 60 °C corresponded to APMT and type 304SS since they have the highest Cr content. The phase angle measurements in Bode plots showed that all the alloys were protected by a passive film, which was probably a surface Cr-rich oxide [17]. No studies were conducted to determine the thickness and composition of the passive film developed on APMT and C26M in near-neutral pH NaCl solutions. It is assumed that this film would have the characteristics of any other stainless steel with the equivalent amount of Cr.

7.3. Passive Behavior in Air under Dry Cask Storage

Dry cask storage is the next storage step in the fuel cycle after the used fuel bundles have been cooled (their radioactivity has been reduced) in cooling pools. The dried-up used fuel bundles would be placed in stainless steel cylinders and hermetically sealed. The steel cylinders with the used fuel would later be placed in vertical or horizontal concrete casks with proper openings for ventilation and air cooling by natural convection. During cask storage, the fuel bundles would be dry at temperatures normally not much higher than 100 °C. It is expected that due to this relatively low exposure temperature, all diffusion processes contributing to surface oxidation would be kinetically slow and non-threatening to the integrity of the cladding for up to 100 years. Surface films on the surface would likely be thin Cr-rich oxides typical of stainless steels.

7.4. Effect of FeCrAl Alloy Composition on Dissolution in Mineral Acids

After extended dry cask storage, the used fuel management policy of each country determines if some of the fuel can be reprocessed or go directly to a geologic repository. In fuel reprocessing or recycling, the fuel pellets themselves need to be separated from the cladding and then the unused fissionable material can be extracted from the dissolved fuel pellets. The way the cladding is separated from the fuel pellets will depend on the nature of the cladding. There is an established reprocessing protocol for claddings based on the element Zr, but recycling process methods still need to be formalized for future FeCrAl claddings. It was shown that C26M dissolves at corrosion rates higher than 100 mpy when exposed to 1 M hydrochloric acid and 0.5 M sulfuric acid at 30 °C. If the temperature is raised to 90 °C, the corrosion (dissolution) rate may increase by more than 100 times [27]. The dissolution rate for APMT is lower than for C26M probably because of its higher Cr content. In 1 M nitric acid solutions, the dissolution rates for both alloys are much lower, probably because nitric acid promotes the passivation of these stainless Cr-containing alloys. Electrochemical impedance spectroscopy tests of APMT and C26M in the three studied acids corroborated the immersion test studies. The most aggressive acid was HCl, followed by H₂SO₄, and the least aggressive was HNO₃. Bode plots of the phase angle showed that both APMT and C26M as well as type 304SS did not have a passivating film on the surface when in the presence of 1 M HCl at 30 °C. In the presence of 1 M HNO₃ at 30 °C, the strongest passivation was for APMT. The composition and thickness of the passive film on APMT was never analyzed.

8. Conclusions

FeCrAl alloys are being considered for nuclear applications due to their unique characteristics of good mechanical properties and their environmental resistance in a large range of temperatures from ambient temperature to 1000 °C or higher.

The unique corrosion degradation resistance is that FeCrAl alloys can develop the right type of surface oxide to resist the environmental conditions to which it is exposed.

Under light water reactor conditions at near 300 °C, for example, the FeCrAl can have a micrometer-range-thick surface oxide rich in Fe under oxidizing conditions or a nanometer-range-thick oxide rich in Cr under reducing conditions.

In air or steam at temperatures higher than 1000 °C, the protective surface oxide is a one-micrometer-thick layer of alpha alumina. The alumina formed on the FeCrAl cladding surface can protect the component from catastrophic oxidation and failure under loss of coolant accident (LOCA) conditions.

The combination of the good mechanical properties and oxidation resistance of FeCrAl alloys would also make them candidates for future reactors which operate at temperatures higher than 650 °C.

Author Contributions: Conceptualization, H.Q. and R.B.R.; methodology, L.Y. and R.B.R.; validation, H.Q., L.Y. and R.B.R.; formal analysis, L.Y. and R.B.R.; investigation, M.L., L.Y. and R.B.R.; resources, R.B.R.; data curation, M.L. and L.Y.; writing—original draft preparation, H.Q., L.Y. and R.B.R.; writing—review and editing, H.Q. and R.B.R.; visualization, H.Q. and R.B.R.; supervision, R.B.R.; project administration, R.B.R.; funding acquisition, R.B.R. All authors have read and agreed to the published version of the manuscript.

Funding: The funding support from Global Nuclear Fuel (GNF), GE Vernova Advanced Research (GEVAR), and GE Hitachi Nuclear is gratefully acknowledged. This material is based upon work supported by the Department of Energy under Award Number DE-NE0009047.

Data Availability Statement: Data can be made available upon reasonable requests to the corresponding authors.

Conflicts of Interest: All the authors were employed by General Electric Vernova Advanced Research. The authors declare that the research was conducted in the absence of any commercial or financial relationships that could be construed as a potential conflict of interest. This material is based upon work supported by the Department of Energy under Award Number DE-NE0009047. This report was prepared as an account of work sponsored by an agency of the United States Government. Neither the United States Government nor any agency thereof, nor any of their employees, makes any warranty, express or implied, or assumes any legal liability or responsibility for the accuracy, completeness, or usefulness of any information, apparatus, product, or process disclosed, or represents that its use would not infringe privately owned rights. Reference herein to any specific commercial product, process, or service by trade name, trademark, manufacturer, or otherwise does not necessarily constitute or imply its endorsement, recommendation, or favoring by the United States Government or any agency thereof. The views and opinions of the authors expressed herein do not necessarily state or reflect those of the United States Government or any agency thereof. The funder was not involved in the study design, collection, analysis, interpretation of the data, the writing of this article, or the decision to submit it for publication.

References

1. Huang, S.; Dolley, E.; An, K.; Yu, D.; Crawford, C.; Othon, M.A.; Spinelli, I.; Knussman, M.P.; Rebak, R.B. Microstructure and Tensile Behavior of Powder Metallurgy FeCrAl Accident Tolerant Fuel Cladding. *J. Nucl. Mater.* **2022**, *560*, 153524. [[CrossRef](#)]
2. Yin, L.; Jurewicz, T.B.; Larsen, M.; Drobnjak, M.; Graff, C.C.; Lutz, D.R.; Rebak, R.B. Uniform Corrosion of FeCrAl Cladding Tubing for Accident Tolerant Fuels in Light Water Reactors. *J. Nucl. Mater.* **2021**, *554*, 153090. [[CrossRef](#)]
3. Qu, H.J.; Abouelella, H.; Chikhalikar, A.S.; Rajendran, R.; Roy, I.; Priedeman, J.; Umretiya, R.; Hoffman, A.; Wharry, J.P.; Rebak, R. Effect of Nickel on the Oxidation Behavior of FeCrAl Alloy in Simulated PWR and BWR Conditions. *Corros. Sci.* **2023**, *216*, 111093. [[CrossRef](#)]
4. Chikhalikar, A.; Roy, I.; Abouelella, H.; Umretiya, R.; Hoffman, A.; Larsen, M.; Rebak, R.B. Effect of Aluminum on the FeCr(Al) Alloy Oxidation Resistance in Steam Environment at Low Temperature (400 °C) and High Temperature (1200 °C). *Corros. Sci.* **2022**, *209*, 110765. [[CrossRef](#)]

5. Rajendran, R.; Chikhalikar, A.S.; Roy, I.; Abouelella, H.; Qu, H.J.; Umretiya, R.V.; Hoffman, A.K.; Rebak, R.B. Effect of Aging and α' Segregation on Oxidation and Electrochemical Behavior of FeCrAl Alloys. *J. Nucl. Mater.* **2024**, *588*, 154751. [[CrossRef](#)]
6. Roy, I.; Abouelella, H.; Rajendran, R.; Chikhalikar, A.S.; Larsen, M.; Umretiya, R.; Hoffman, A.; Rebak, R. Effect of Al Concentration on Fe-17Cr Alloy during Steam Oxidation at 400 °C. *Corros. Sci.* **2023**, *217*, 111135. [[CrossRef](#)]
7. Rebak, R.B.; Yin, L.; Zhang, W.; Umretiya, R.V. Effect of the Redox Potential on the General Corrosion Behavior of Industrial Nuclear Alloys. *J. Nucl. Mater.* **2023**, *576*, 154257. [[CrossRef](#)]
8. Jurewicz, T.; Rebak, R. Electrochemistry of FeCrAl Fuel Cladding in High Temperature Water. *Trans. Am. Nucl. Soc.* **2018**, *118*, 17–21.
9. Terrani, K.A. Accident Tolerant Fuel Cladding Development: Promise, Status, and Challenges. *J. Nucl. Mater.* **2018**, *501*, 13–30. [[CrossRef](#)]
10. Field, K.G.; Snead, M.A.; Yamamoto, Y.; Terrani, K.A. *Handbook on the Material Properties of FeCrAl Alloys for Nuclear Power Production Applications (FY18 Version: Revision 1)*; Oak Ridge National Lab. (ORNL): Oak Ridge, TN, USA, 2018.
11. Sakamoto, K.; Miura, Y.; Ukai, S.; Oono, N.H.; Kimura, A.; Yamaji, A.; Kusagaya, K.; Takano, S.; Kondo, T.; Ikegawa, T.; et al. Development of Accident Tolerant FeCrAl-ODS Fuel Cladding for BWRs in Japan. *J. Nucl. Mater.* **2021**, *557*, 153276. [[CrossRef](#)]
12. Qu, Z.; Meng, C.; Huang, J.; Mei, Y.; Zhang, Y.; Ma, J.; Liu, W.; Wang, H.; He, X. Mechanistic Study of Incipient Corrosion for Nuclear Grade Lean-Cr FeCrAl Alloys in a Simulated PWR Environment. *Mater. Des.* **2023**, *230*, 111948. [[CrossRef](#)]
13. Terrani, K.A.; Pint, B.A.; Kim, Y.-J.; Unocic, K.A.; Yang, Y.; Silva, C.M.; Meyer, H.M.; Rebak, R.B. Uniform Corrosion of FeCrAl Alloys in LWR Coolant Environments. *J. Nucl. Mater.* **2016**, *479*, 36–47. [[CrossRef](#)]
14. Raiman, S.S.; Field, K.G.; Rebak, R.B.; Yamamoto, Y.; Terrani, K.A. Hydrothermal Corrosion of 2nd Generation FeCrAl Alloys for Accident Tolerant Fuel Cladding. *J. Nucl. Mater.* **2020**, *536*, 152221. [[CrossRef](#)]
15. Ning, F.; Wang, X.; Yang, Y.; Tan, J.; Zhang, Z.; Jia, D.; Wu, X.; Han, E.-H. Uniform Corrosion Behavior of FeCrAl Alloys in Borated and Lithiated High Temperature Water. *J. Mater. Sci. Technol.* **2021**, *70*, 136–144. [[CrossRef](#)]
16. Yamashita, S.; Ioka, I.; Nemoto, Y.; Kawanishi, T.; Kurata, M.; Kaji, Y.; Fukahori, T.; Nozawa, T.; Sato, D.; Murakami, N.; et al. Overview of Accident-Tolerant Fuel R&D Program in Japan. In Proceedings of the 14th International Nuclear Fuel Cycle Conference, GLOBAL 2019 and Light Water Reactor Fuel Performance Conference, TOP FUEL 2019, Seattle, WA, USA, 22–27 September 2019.
17. Rebak, R.; Jurewicz, T.; Larsen, M.; Sakamoto, K. Immersion Testing of FeCrAl Tubes under Simulated Light Water Nuclear Reactor Normal Operation Conditions. In Proceedings of the Top Fuel 2019 Conference, Seattle, WA, USA, 22–27 September 2019.
18. Jiang, G.; Xu, D.; Feng, P.; Guo, S.; Yang, J.; Li, Y. Corrosion of FeCrAl Alloys Used as Fuel Cladding in Nuclear Reactors. *J. Alloys Compd.* **2021**, *869*, 159235. [[CrossRef](#)]
19. Was, G.S.; Allen, T.R. Corrosion in Advanced Nuclear Reactors. *Electrochem. Soc. Interface* **2021**, *30*, 57. [[CrossRef](#)]
20. Qu, H.J.; Chikhalikar, A.S.; Abouelella, H.; Roy, I.; Rajendran, R.; Nagothi, B.S.; Umretiya, R.; Hoffman, A.K.; Rebak, R.B. Effect of Molybdenum on the Oxidation Resistance of FeCrAl Alloy in Lower Temperature (400 °C) and Higher Temperature (1200 °C) Steam Environments. *Corros. Sci.* **2024**, *229*, 111870. [[CrossRef](#)]
21. Pint, B.A. Performance of FeCrAl for Accident-Tolerant Fuel Cladding in High-Temperature Steam. *Corros. Rev.* **2017**, *35*, 167–175. [[CrossRef](#)]
22. Qian, L.; Liu, Y.; Huang, T.; Chen, W.; Du, S.; Yin, C.; Xiong, Q. Research Progress in High-Temperature Thermo-Mechanical Behavior for Modelling FeCrAl Cladding under Loss-of-Coolant Accident Condition. *Prog. Nucl. Energy* **2023**, *164*, 104848. [[CrossRef](#)]
23. Yan, Y.; Harp, J.; Coq, A.L.; Massey, C.; Linton, K. High-Temperature Steam Oxidation Study of Irradiated FeCrAl Defueled Specimens. *J. Nucl. Mater.* **2024**, *590*, 154868. [[CrossRef](#)]
24. Rebak, R.B. *Accident-Tolerant Materials for Light Water Reactor Fuels*; Elsevier: Amsterdam, The Netherlands, 2020.
25. Rebak, R.B.; Gupta, V.K.; Larsen, M. Oxidation Characteristics of Two FeCrAl Alloys in Air and Steam from 800 °C to 1300 °C. *JOM* **2018**, *70*, 1484–1492. [[CrossRef](#)]
26. Lipkina, K.; Hallatt, D.; Geiger, E.; Fitzpatrick, B.W.N.; Sakamoto, K.; Shibata, H.; Piro, M.H.A. A Study of the Oxidation Behaviour of FeCrAl-ODS in Air and Steam Environments up to 1400 °C. *J. Nucl. Mater.* **2020**, *541*, 152305. [[CrossRef](#)]
27. Rebak, R.B.; Yin, L.; Jurewicz, T.B.; Hoffman, A.K. Acid Dissolution Behavior of Ferritic FeCrAl Tubes Candidates for Nuclear Fuel Cladding. *Corrosion* **2021**, *77*, 1321–1331. [[CrossRef](#)]

Disclaimer/Publisher's Note: The statements, opinions and data contained in all publications are solely those of the individual author(s) and contributor(s) and not of MDPI and/or the editor(s). MDPI and/or the editor(s) disclaim responsibility for any injury to people or property resulting from any ideas, methods, instructions or products referred to in the content.